Supplementary Information for:
Native Serotonin Membrane Receptors Recognize 5-Hydroxytryptophan-Functionalized Substrates: Enabling Small-Molecule Recognition

Amit Vaish,[†] Mitchell J. Shuster,[‡] Sarawut Cheunkar,[§] Yogesh S. Singh,[§] Paul S. Weiss,[‡,§,∥,¶,▽] and Anne M. Andrews*[,§,⊥,∥,#,▽]

[†]Department of Bioengineering, [‡]Department of Physics, [§]Department of Chemistry, [⊥]Department of Veterinary & Biomedical Sciences, [∥]Huck Institutes of the Life Sciences, Pennsylvania State University, University Park, Pennsylvania 16802, [¶]Departments of Chemistry and Biochemistry, [#]Department of Psychiatry, and [▽]California NanoSystems Institute, University of California, Los Angeles, Los Angeles, California 90095

Preparation and functionalization of SAMs

Mixed monolayers were prepared on gold surfaces by co-deposition of 1 mM solutions in ethanol (EtOH) of 23-(9-mercaptononyl)-3,6,9,12,15,18,21-heptaoxatricosanoic acid (HEG) and 1-(9-mercaptononyl)-3,6,9-trioxaundecan-11-ol (TEG) in a 95:5 molar ratio for 12 h (Figure S1). Self-assembled monolayers (SAMs) were rinsed with EtOH and dried under a stream of nitrogen. Monolayers terminated with oligo(ethylene glycol) have been shown to be non-reactive and to resist nonspecific biomolecule adsorption *(1-6)*. In a previous study, we used insertion-directed self-assembly to place tethers into pre-existing SAMs prior to functionalization to achieve dilute probe surface coverage *(7)*. However, the present studies using gold-coated quartz crystals in combination with insertion self-assembly did not produce probe-functionalized substrates with reproducible biomolecule binding characteristics across batches of QCM crystals. We hypothesize that differences in Au deposition on quartz crystals by the manufacturer, which

lead to variability in SAM defects and, consequently, insertion of tethers, underlie this observation. To circumvent this, we utilized co-deposition from solution to produce dilute coverage of tethers in the present experiments. We have observed, in agreement with other published studies, that using low molar fractions of tether molecules (<0.08), as part of a mixed component SAM system whose components have a low probability of phase separation, results in small-molecule dilution that facilitates recognition by large biomolecule binding partners while minimizing non-specific interactions.

Dilute surfaces functionalized with 5-hydroxytryptophan (5-HTP) were synthesized as

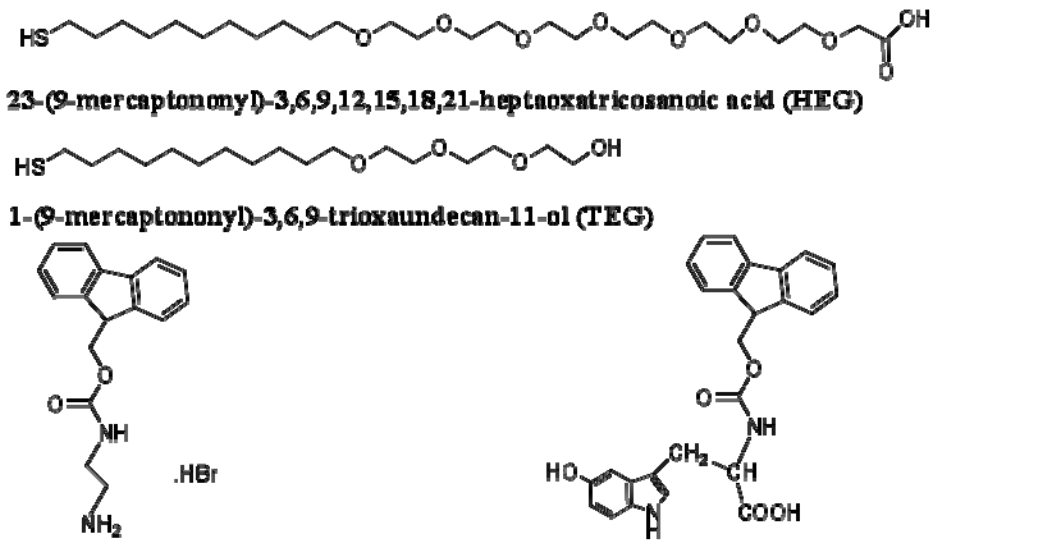

Figure S1. Structures of the compounds used in the assembly and synthesis of serotonin- and 5-HTP-functionalized monolayers. Thiols used for self-assembly are HEG and TEG (top). For 5-HTP, FMOC-protected 1,2-diaminoethane (FMOC-DAE) was used as a linker for covalent attachment of FMOC-protected 5-HTP (FMOC-5-HTP) to dilute HEG tethers.

shown in Figure S-2. Carboxyl-terminated thiols in mixed monolayers (Figure S2, step **i**) were ester-activated by exposure to aqueous solutions of 75 mM *N*-ethyl-*N*-(dimethylaminopropyl)-

carbodiimide (EDC) and 15 mM *N*-hydroxysulfosuccinimide (NHSS) for 1 h (Figure S2, step **ii**). Amide bonds were then formed between the primary amines of the linker *N*-fluorenylmethoxycarbonyl-1,2-diaminoethane hydrobromide (FMOC-DAE; 10 mM in dimethylformamide (DMF); Figure S1) and the activated carboxyl groups on the monolayer surfaces (Figure S2, step **iii**) during a 12 h incubation.

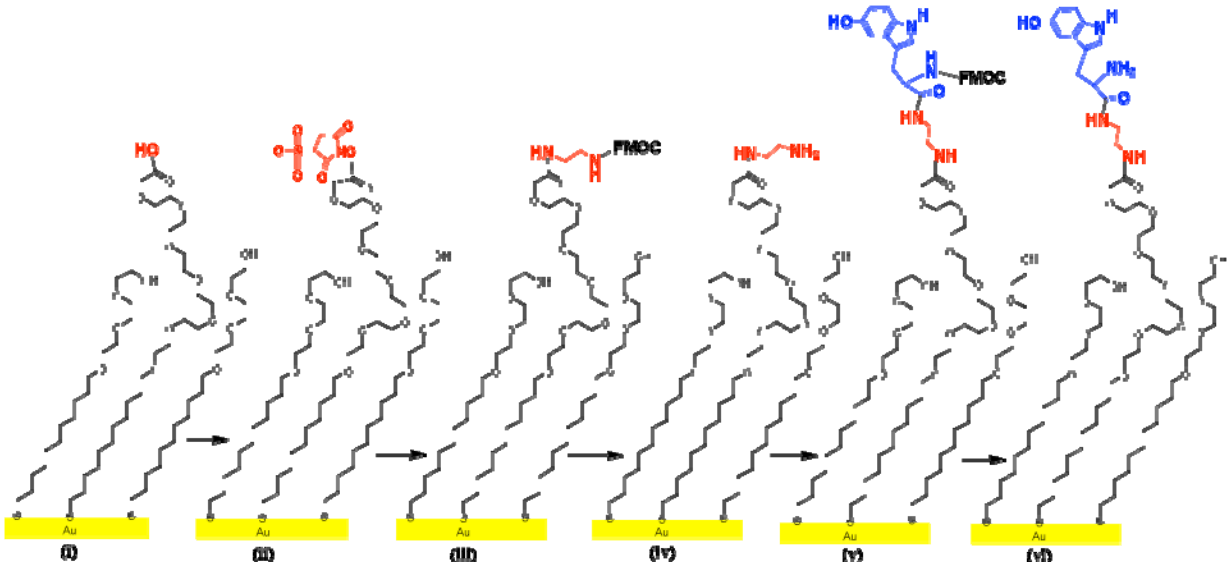

Figure S2. Schematic of the stepwise covalent immobilization of 5-HTP on mixed SAMs. **(i)** Mixed SAM formation on a gold surface by solution deposition of TEG:HEG at a nominal 95:5 molar ratio. **(ii)** Activation of carboxyl-terminated tethers by esterification with NHSS. **(iii)** Attachment of FMOC-DAE linkers to ester-activated tethers. **(iv)** Deprotection of diaminoethane linkers. **(v)** Covalent attachment of FMOC-5-HTP (activated ester of FMOC-5-HTP not shown). **(vi)** Deprotection to produce covalently bound 5-HTP. (Relative proportions of the SAM components are not representative.)

The FMOC protecting groups were removed from surface-attached linkers by immersion in 20% piperidine in DMF for 20 min, resulting in amine-functionalized surfaces (Figure S2, step **iv**). Next, 15 mM 9-fluorenylmethoxycarbonyl-5-hydroxy-L-tryptophan (FMOC-L-5-HTP) or

9-fluorenylmethoxycarbonyl-5-hydroxy-DL-tryptophan (FMOC-DL-5-HTP) (Figure S1) was conjugated to amine-functionalized surfaces in the presence of 10 mM *N*-hydroxysuccinimide (NHS), 1 mM diisopropylcarbodiimide (DIC), and 30 mM EDC in DMF (Figure S2, step **v**) (5 h incubation). Finally, deprotection was carried out a second time to generate dilute 5-HTP-functionalized SAMs (Figure S2, step **vi**) *(8)*. Samples were rinsed with DMF, followed by 50:50 EtOH:deionized H_2O, followed by deionized H_2O, and finally EtOH, and dried under a stream of nitrogen. Surfaces functionalized with serotonin were prepared as previously described *(7)* with the exception that monolayers were formed by self-assembly of 95:5 TEG:HEG co-deposited from solution, as described above.

Surface characterization

To prepare samples specifically for analysis and optimization of surface chemistry, 100 Å Cr followed by 1000 Å Au was deposited in house by electron-beam evaporation (Kurt J. Lesker, Clairton, PA) on thermally oxidized Si substrates (Silicon Quest, Santa Clara, CA) followed by SAM formation and dilute 5-HTP-functionalization, as described above and in Figure S2. X-ray photoelectron spectroscopy (XPS) measurements were made using a Kratos Axis Ultra XPS system (Kratos Analytical, Chestnut Ridge, NY), a monochromatic Al k_α x-ray source (20 mA, 14 kV) with a 200-μm circular spot size, and ultrahigh vacuum (10^{-9} Torr). High-resolution spectra of the C 1s, N 1s, O 1s, S 2p, and Au 4f regions were acquired at a pass energy of 40 eV. All binding energies were referenced to the Au $4f_{7/2}$ peak at 84.0 eV. Each of the acquired spectra was an average of scans taken at five different spots on each sample. To quantify the nitrogen content, the normalized area under the peak in the N 1s region was obtained for each sample by dividing individual sample peak areas by the

average peak area of diaminoethane-functionalized SAMs (n=3). Infrared reflectance absorption spectrometry (IRRAS) was carried out using a Thermo Nicolet 6700 FT-IR spectrometer (Thermo Electron Corp., Madison, WI) via reflectance mode and infrared light incident at 84° relative to the surface normal. Spectra are the result of 1024 scans. A perdeuterated decanethiol monolayer spectrum scanned under identical conditions was used for background subtraction.

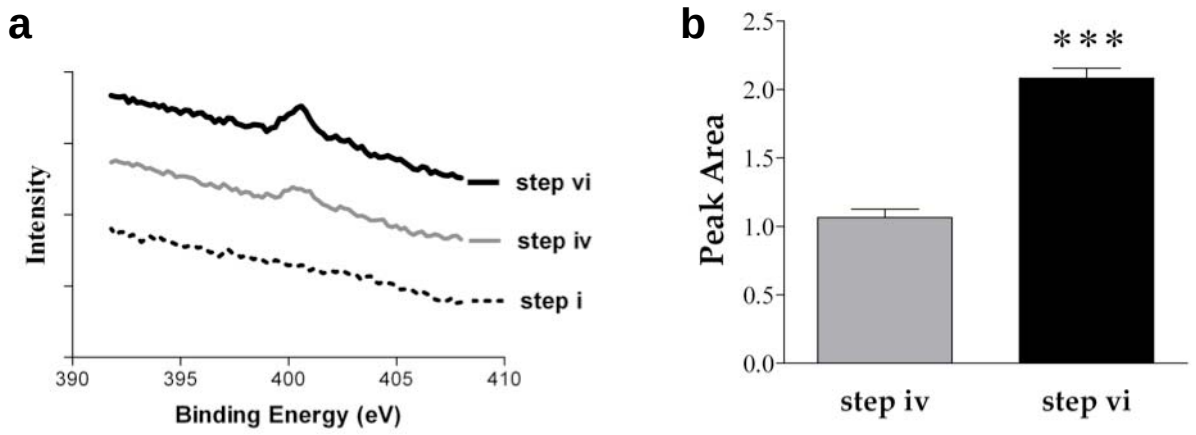

Figure S3. Characterization of surface functionalization by x-ray photoelectron spectroscopy. **(a)** Representative XPS spectra of the N 1s region from a mixed self-assembled monolayer (SAM) co-deposited from a 95:5 molar ratio of TEG:HEG (step **i**, Figure S2); SAM with diaminoethane linkers attached and following deprotection (step **iv**, Figure S2); and SAM further derivatized with 5-HTP and following deprotection (step **vi**, Figure S2). **(b)** The peak areas indicate that twice the amount of nitrogen is present after step **vi** compared to step **iv**, consistent with the stoichiometry of the surface chemistry. ($t(4)=11$;***$P<0.001$ vs. B)

X-ray photoelectron spectroscopy was used to determine the changes in nitrogen content of SAMs after steps **iv** and **vi** (Figure S2) during the assembly and synthesis of 5-HTP-functionalized surfaces. Figure S3A shows the N 1s region from representative high-resolution XPS spectra. Figure S3B depicts the normalized mean N 1s areas under the peak for

three separate samples at each synthesis step. Nitrogen was not detected on the initial SAM surfaces prepared by solution co-deposition of a 95:5 molar ratio of TEG:HEG. Addition of FMOC-DAE (step **iii**, Figure S2) followed by deprotection (step **vi**, Figure S2) resulted in XPS spectra in which N 1s peaks were detected at a binding energy of 400 eV. Primary and secondary amines have N 1s binding energies in the range of 399 to 402 eV. Formation of a second amide bond (step **v**, Scheme 1) with FMOC-5-HTP followed by deprotection (step **vi**, Figure S2) resulted in a quantitative doubling of the amount of nitrogen detected by XPS, as illustrated by the increase in the mean normalized N 1s peak area (Figure S3B). These and other data indicate that the coupling of 5-HTP, which contains two nitrogen atoms per molecule, to 1,2-diaminoethane linkers also having two nitrogen atoms per molecule, occurs

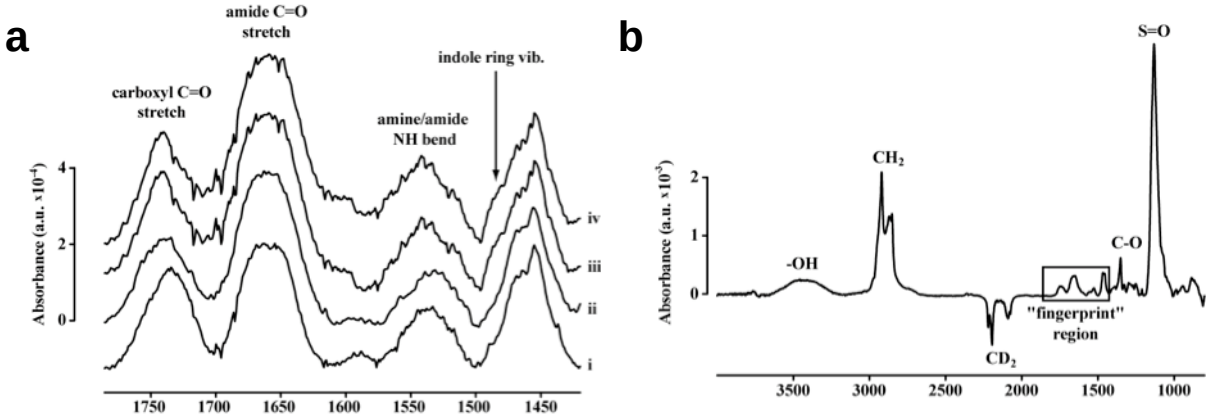

Figure S4. **Surface functionalization with 5-hydroxytryptophan monitored by infrared reflectance spectroscopy. (a)** A SAM with the FMOC-DAE linkers attached (i) (step **iii**, Figure S2), following deprotection (ii) (step **iv**, Figure S2), after SAM derivatization with FMOC-5-HTP (iii) (step **v**, Figure S2), and following deprotection (iv) (step **vi**, Figure S2). Spectra are offset for clarity. **(b)** A representative full IRRAS spectrum after step **vi**, Figure S2.

stoichiometrically.

In previous studies on 5-HT-functionalized surfaces, we used IRRAS to provide information at individual steps about assembly and synthesis *(7)*. Here, we similarly monitored sequential changes in surface chemistry of 5-HTP-functionalized surfaces. In Figure S4A, the appearance of a carbonyl peak at 1663 cm^{-1} is indicative of the presence of amide carbonyls resulting from 1,2-diaminoethane **(i)** attachment and conjugation with 5-HTP **(iii)**. However, this peak cannot be used quantitatively as an indicator of the progression of the surface chemistry because the intensity of IRRAS peaks varies due to molecular orientation effects.

Because of the low coverage of probe-functionalized tethers in these SAMs, and possible orientation effects, spectral peaks for the FMOC protecting groups could not be identified directly in the IR spectra. The appearance and disappearance of peaks indicative of primary amine groups on the surface might be used as a partial indicator for the presence and absence of the FMOC group, as removal of this protecting group produces a primary amine. However, as illustrated in Figure S4A, resolving the different peaks resulting from primary vs. secondary amines is difficult. Generally, characteristic peaks for the symmetric and asymmetric stretches of primary amines are observed in the 3250 to 3550 cm^{-1} range, but spectral interference due to the broad hydrogen-bonded hydroxyl peak from the hydroxyl-terminated monolayer obscures amine peak identification in this region. Similarly, characteristic peaks between 1000 and 1300 cm^{-1} were not suitable for tracking the formation of primary amines because of the many carbonyl peaks generated by the oligo(ethylene glycol) and hydroxyl-terminated SAM. This is illustrated in Figure S4B. Additionally, amine peaks, especially those in the 1400 to 1700 cm^{-1} region, are highly variable, as has been noted *(9, 10)*.

Peaks from ring structures indicative of the presence of an indole on the surface suffer from limitations similar to those associated with identifying primary amines. However, spectra **iii**

and **iv** in Figure S4A show a peak at 1488 cm^{-1} likely due to an indole ring vibration that is diagnostic of 5-HTP. This peak generally manifests as a shoulder of variable intensity on the strong 1465 cm^{-1} methylene (CH_2) deformation due to the C_{11} backbone of the monolayer. In particular, this indole shoulder may be absent in the presence of the FMOC protecting group. Regardless, the IRRAS and XPS data together indicate that 5-HTP becomes covalently bound via a diaminoethane linker to dilute carboxyl groups on HEG-terminated tethers in mixed SAMs.

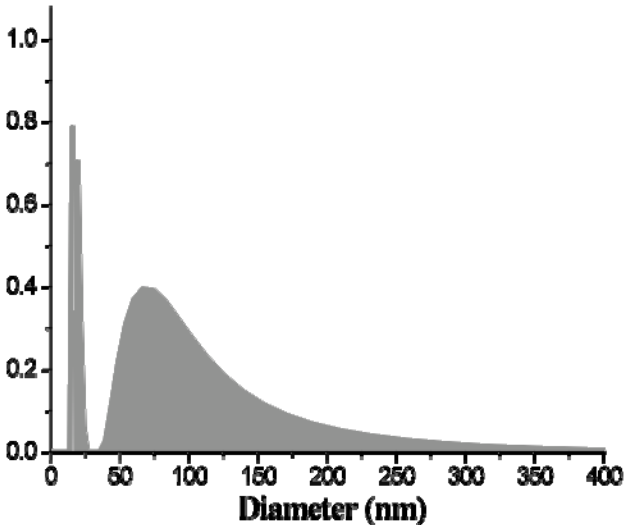

Figure S5. Membrane vesicles are distributed over of a range of sizes. Diameters of membrane-associated 5-HT_7 receptor-containing vesicles were measured by dynamic light scattering revealing that the membrane preparations consisted of a range of vesicle sizes that distribute bimodally. Larger vesicles had a mean diameter of 95 nm and smaller vesicles had a mean diameter of 18 nm.

Vesicle characterization

Membrane-associated receptor preparations containing 5-HT_7 receptors were analyzed by dynamic light scattering (DLS) to determine the size distributions of the membrane vesicles. As shown in Figure S5, the analysis indicated that membrane vesicles exhibited a bimodal distribution with smaller vesicles having a mean diameter of 18 nm and larger vesicles having a mean diameter of 95 nm. Membrane preparations containing the other receptor proteins studied showed similar bimodal size distributions. A previous study by Vidic *et al.* on membrane preparations containing olfactory receptors reported a similar wide range of vesicle sizes *(11)*.

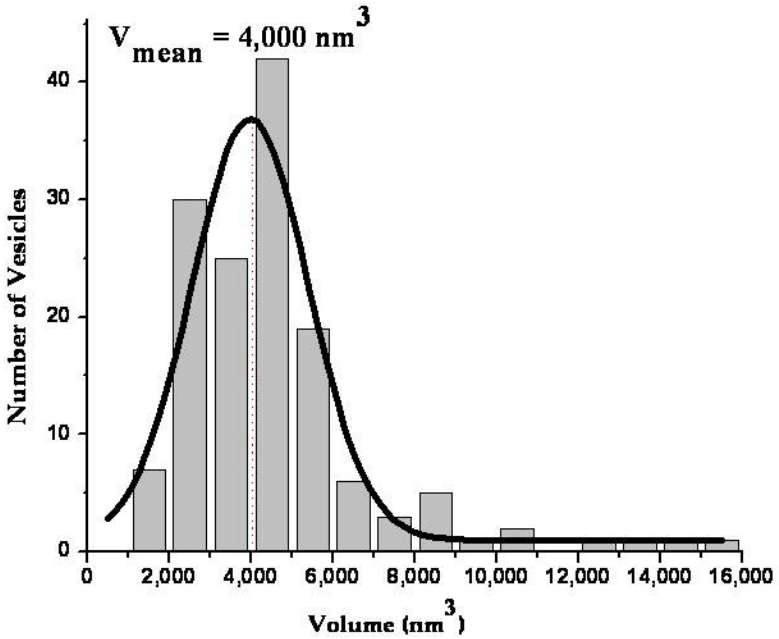

Figure S6. Gaussian fit for the volume histogram of surface-captured vesicles from the AFM data shown in Figure 4. Volumes for 142 vesicles distributed over six representative surfaces were determined. The mean vesicle volume of 4,000 nm^3 determined by AFM corresponds well with the mean volume (3,000 nm^3) of the smaller population of vesicles observed by DLS (Supplemental Figure S5).

Receptor binding schematic

The space-filling model of the 5-HTP-functionalized SAM was designed using ArgusLab Molecular Modeling and Drug Docking software (Seattle, WA). The ball and stick model of the plasma membrane and the space-filling model of the human 5-HT_{1B} receptor were generated using their respective RCSB Protein Data Bank (PDB) files and the Swiss PDB viewer. Carbon, oxygen, nitrogen, and sulfur atoms are depicted in gray, red, blue, and yellow, respectively. The PDB file for the plasma membrane was generated by Heller and coworkers using molecular dynamics simulation *(12)*. The PDB file for the human 5-HT_{1B} receptor (PDB id 2G1X) was submitted by Pradhan and coworkers to the Protein Data Bank and was generated by theoretical modeling based on the crystal structure of the G-protein receptor bovine rhodopsin.

Fifteen different serotonin receptors (and subunits) have been molecularly identified, 13 of which are G-protein-coupled receptors *(13)*. The human 5-HT_{1B} receptor in the schematic is the only serotonin G-protein-coupled receptor for which a PDB file is publically available. Extracellular and intracellular domains were identified using the sequence annotation feature in the Protein Knowledge base (www.uniprot.org/uniprot/P28222). This schematic is intended to approximate the respective sizes of tethered 5-HTP relative to the SAM components and a typical membrane-associated G-protein-coupled serotonin receptor. Due to lack of crystallographic data for all serotonin receptors, including the receptors investigated here, specific assumptions about the structures of the 5-HT_{1B}, 5-HT_7, and 5-HT_{1A} receptor cannot yet be made.

Chemicals

Oligo(ethylene glycol) alkanethiols were purchased from Toronto Research Chemicals (Toronto, ON). 5-Hydroxytryptophan, FMOC-DAE, EDC, DIC, NHS, DMF, piperidine, and bovine serum albumin were obtained from Sigma-Aldrich (St. Louis, MO). FMOC-L-5-HTP and FMOC-DL-5-HTP were purchased from Anaspec (San Jose, CA). NHSS was obtained from Pierce Biotechnology (Rockford, IL). Commercial grade EtOH was obtained from Pharmaco-AAPER (Brookfield, CT). Human recombinant membrane receptors (5-HT_7, 5-HT_{1A}, $GABA_{B1b}$, and D1) were purchased from PerkinElmer (Waltham, MA). Antibodies (rabbit anti-5-HTP and rabbit anti-immunoglobulin-G (IgG)) were procured from Millipore (Temecula, CA).

References

1. Prime, K. L., and Whitesides, G. M. (1991) Self-assembled organic monolayers: model systems for studying adsorption of proteins at surfaces, *Science 252*, 1164-1167.
2. Lee, K. B., Park, S. J., Mirkin, C. A., Smith, J. C., and Mrksich, M. (2002) Protein nanoarrays generated by dip-pen nanolithography, *Science 295*, 1702-1705.
3. Hodneland, C. D., Lee, Y. S., Min, D. H., and Mrksich, M. (2002) Selective immobilization of proteins to self-assembled monolayers presenting active site-directed capture ligands, *Proc. Natl. Acad. Sci. U.S.A. 99*, 5048-5052.
4. Lahiri, J., Isaacs, L., Tien, J., and Whitesides, G. M. (1999) A strategy for the generation of surfaces presenting ligands for studies of binding based on an active ester as a common reactive intermediate: a surface plasmon resonance study, *Anal. Chem. 71*, 777-790.
5. Mrksich, M., Grunwell, J. R., and Whitesides, G. M. (1995) Biospecific adsorption of carbonic-anhydrase to self-assembled monolayers of alkanethiolates that present benzenesulfonamide groups on gold, *J. Am. Chem. Soc. 117*, 12009-12010.
6. Mrksich, M., Dike, L. E., Tien, J., Ingber, D. E., and Whitesides, G. M. (1997) Using microcontact printing to pattern the attachment of mammalian cells to self-assembled monolayers of alkanethiolates on transparent films of gold and silver, *Exp. Cell Res. 235*, 305-313.
7. Shuster, M. J., Vaish, A., Szapacs, M. E., Anderson, M. E., Weiss, P. S., and Andrews, A. M. (2008) Biospecific recognition of tethered small molecules diluted in self-assembled monolayers, *Adv. Mat. 20*, 164-167.
8. Rawsterne, R. E., Todd, S. J., Gough, J. E., Farrar, D., Rutten, F. J., Alexander, M. R., and Ulijn, R. V. (2007) Cell spreading correlates with calculated logP of amino acid-modified surfaces, *Acta. Biomater. 3*, 715-721.
9. Socrates, G. (2001) *Infrared and Raman Characteristic Group Frequencies: Tables and Charts*, 3rd ed., John Wiley & Sons, Inc., New York.
10. Hooper, A. E., Werho, D., Hopson, T., and Palmer, O. (2001) Evaluation of amine- and amide-terminated self-assembled monolayers as 'Molecular glues' for Au and SiO2 substrates, *Surf. Interface Anal. 31*, 809-814.
11. Vidic, J. M., Grosclaude, J., Persuy, M. A., Aioun, J., Salesse, R., and Pajot-Augy, E. (2006) Quantitative assessment of olfactory receptors activity in immobilized nanosomes: a novel concept for bioelectronic nose, *Lab Chip 6*, 1026-1032.
12. Heller, H., Schaefer, M., and Schulten, K. (1993) Molecular-dynamics simulation of a bilayer of 200 lipids in the gel and in the liquid-crystal phases, *J. Phys. Chem. 97*, 8343-8360.
13. Hensler, J. G. (2006) Serotonin, In *Basic Neurochemistry: Molecular, Cellular, and Medical Aspects* (Siegel, G. J., Albers, R. W., Brady, S. T., and Price, D. L., Eds.), pp 227-248, Elsevier Academic Press, New York.